Computer Assisted Methods in Engineering and Science
30(3): 347–367, 2023, doi: 10.24423/cames.654

This article belongs to the *Special Issue on Digital Twin Empowered Internet of Intelligent Things for Engineering Cyber-Physical Human Systems* edited by C. Venkatesan, Y.-D. Zhang, Q. Xin

Enhanced Design and Analysis of the Microcantilever-Based Bio-Sensor to Detect Carcinoembryonic Antigen Tumor Biomarkers

Khalid Mohd IBRAHIMI[1)*], Rajagopal KUMAR[1)], Writtick PAKHIRA[1)], Fenil C. PANWALA[2)]

[1)] *Department of Electronics and Instrumentation Engineering, National Institute of Technology, Nagaland, Dimapur, India; e-mails: rajagopal.kumar4@gmail.com, writtickpakhira@gmail.com*

[2)] *Department of Electronics and Instrumentation Engineering, Siddaganga Institute of Technology, Tumakuru, Karnataka, India; e-mail: fenilpanwala68@gmail.com*

[*] *Corresponding Author e-mail: khalid11july@gmail.com*

Frequently, early detection of a malignant condition prevents most premature deaths. In this paper, three new designs are proposed for the microcantilever-based biosensor to detect carcinoembryonic antigen (CEA) tumor biomarkers. CEA is used for several types of human cancers, e.g., lung cancer, pancreatic cancer, breast cancer, ovarian cancer, and gastric cancer, particularly colorectal cancer. The proposed models are designed and the finite element method (FEM) analysis of these biosensors is performed using a COMSOL 5.4 Multiphysics (commercial package) software. Various analyses and comparisons are carried out by utilizing the designs in terms of displacement as well as piezo-resistive output due to an increase in mass of CEA adsorbed onto the surface of the cantilever beam, which is stimulated by applying a pressure range of 0 to 0.2 Pa on to the surface of a cantilever beam. A simulation is performed with the proposed designs by experimenting with different materials for better deflection results. Regarding the results obtained, Design 3, made with Kynar710, gives the highest total deflection of 0.7328 μm. However, a piezo-resistive readout technique is utilized to get the output in mV, and for that, p-silicon (single-crystal, lightly doped) material is used, respectively. Next, 5V is applied to the terminals of the piezo-resistive circuit. Based on the input applied pressure and output mV, the Design 3 made with Kynar710 gives a better sensitivity of 0.13089 [mV/V/Pa] compared to other designs made with other materials.

Keywords: carcinoembryonic antigen, microcantilever, piezoresistive, tumor biomarkers.

1. Introduction

A major reason for premature death in today's world are malignant conditions along with cardiovascular diseases. It has been proven that an effective method

of saving lives is early detection of a malignant condition. Tumor biomarkers are signaling entities produced by a tumor or host in response to a cancer cell. In tumor diagnosis, screening, and efficacy assessment, tumor biomarkers have great practical importance [1]. At different stages of cell development, tumor biomarkers are supposed to be responsible for the development of normal cells or carcinogenesis [2]. This was first described in 1965, and since then, the most well-studied tumor biomarker is a carcinoembryonic antigen [3]. CEA is a human glycoprotein. It is one of the most popular oncofetal antigens that is usually present during placental life. In adults, it occurs in low quantities and is transmitted in high quantities in patients with specific pathologies, especially epithelial tumors [4]. CEA is frequently used as a tumor biomarker for several human cancers, such as lung cancer, pancreatic cancer, breast cancer, ovarian cancer, and gastric cancer, particularly colorectal cancer (CRC) [3]. Therefore, CEA detection is very important in sequential diagnosis, situation monitoring, and clinical assessment of diseases [5–8].

Nowadays, CEA detection and sensor analysis have attracted extensive attention. Micro-electromechanical systems (MEMS)-based device has become a trademarked technology for the 21st century. It can sense, analyze and control all in a single chip device. MEMS device is an evolving tool in several fields of science and technology. There are two salient characteristics of a MEMS-based device: first, the mechanical structure that can be equated to motion, and second, the electrical signal. The biomedical/biological applications of MEMS have attracted significant attention in the past few years. Biosensors are one of the most widely used applications of MEMS in biomedical/biological diagnosis and analysis. With the advancement in the biosensor technology, biosensors attract much attention as instruments for diagnosis and analysis. It is an emerging field that meets people's needs for low-cost, simple, selective, and fast analysis. There are mainly two parts in a biosensor: a bioreceptor (or bio-recognition) component and a transducer. A bioreceptor is a biomolecule that is associated with the target molecule and recognizes it. This bio-recognition is converted into a measurable signal with the help of a transducer [9].

The distinctiveness of a biosensor is that the two different components (i.e., bioreceptor and transducer) are integrated into one single chip to form a single sensor. This blend of components enables one to measure the analyte or target molecules without using any reagent. For example, to measure the glucose concentration in a blood sample, a specific biosensor designed for glucose measurement can be used by just dipping it into the sample. Upadhyaya *et al.* [10] proposed an integrated optical micro ring resonator-based microcantilever sensor for detecting CEA present in the human body. They proposed two types of design, rectangular and triangular shapes, and the effect of geometric variation of the proposed microcantilever sensor was verified by the sensitivity and quality

factor of the cantilever design. They obtained sensitivity and quality factor of 60 nm/MPa and 11 458 for triangular shape, respectively, and 0.01 nm/MPa and 3805 for rectangular shape, respectively. Xiang *et al.* [11] reviewed the aptamer biosensors' use for CEA detection. Two aspects of the aptamer-based biosensors were discussed in detail: optical and electrochemical sensors.

Li *et al.* [12] proposed an array of microcantilever biosensors with a sandwich structure for measuring α-fetoprotein (APF) and CEA simultaneously by using an optical readout technique. The sensitivity of detection for AFP was 0.6 ng/mL and for CEA was 1.3 ng/mL. Pinto *et al.* [13] proposed a system to detect the microRNA-145, which is a cancer-associated biomarker. They proposed the rectangular amorphous silicon (a-Si) cantilevers, about 500 nm thick, 20 μm wide, and 60 μm long, which were fabricated on glass substrates. The capacitive readout technique was used and they found that the minimum detectable tip deflection is 42.8 nm in air and 17.2 nm in water. Lakshmi *et al.* [14] developed a silicon rectangular cantilever beam-based sensor for detecting glucose levels in the blood. They used different readout methods, which were focused on piezoresistive, capacitive and piezoelectric principles in microcantilevers. The piezoresistive readout-based microcantilever offers the best sensitivity and nonlinearity, 5.03×10^{-9} and 30%, respectively. Rotake *et al.* [15] examined the sensitivity and stiffness of a microcantilever with a readout technique of piezoresistive pressure sensor for detecting very small stress developed by the DNA hybridization and immobilization of the antibody. They found the highest sensitivity and stiffness for Au/Cr thin film top layer in gold and silicon dioxide. Andrade *et al.* [16] proposed a cantilever-based biosensor to detect the concentration of miRNA-203 and miRNA-205. They proposed a silicon-based rectangular cantilever, about 450 μm long, 50 μm wide, and 2 μm thick. They used atomic force microscopy (AFM)-based readout technique. They observed that when a target analyte was present on the surface of the cantilever, the average deflections observed were 188 ± 9 nm and 320 ± 20 nm for miRNA-203 and miRNA-205, respectively.

In this paper, three designs of microcantilever (i.e., Design 1, Design 2, and Design 3) are proposed, including a piezoresistive-based readout. Here, p-type piezoresistors are used with a doping density of 1.32×10^{19} $(1/\mathrm{cm}^3)$ because they provide better sensitivity than n-type piezoresistors [17]. The design, optimization, and analysis of microcantilever-based biosensors is made with the help of the FEM module of the COMSOL 5.4 Multiphysics software.

The main objective of the proposed work is to design microcantilevers by keeping the active sensing area equivalent to a rectangular shape design [10], with different geometrical shapes using different materials and applying pressure in the range of 0 to 0.2 Pa on the microcantilever. This range of pressure applied on the cantilever surface acts as the mass of the CEA adsorbed onto the surface of a cantilever beam. Piezoresistive readout techniques are used for taking the

electrical output and a comparative analysis of deflection, von Misses stress, and output voltage. Finally, the conclusion shows better sensitivity based on the output data.

2. Basic theory

The biosensor is a general term used for a whole class of sensors that use a biochemical reaction to determine a specific compound. These are analytical tools that combine the elements biologically sensitive with a chemical or physical transducer to selectively and quantitatively detect existence of specific compounds in a given external environment. MEMS provide a different approach to the recognition of molecular quantities. Cantilever-based sensors using MEMS technologies are alternative future-generation platforms that are easily built wafers of silicon. Figure 1 presents basic elements of the biosensor. Figure 2 shows detection using a microcantilever.

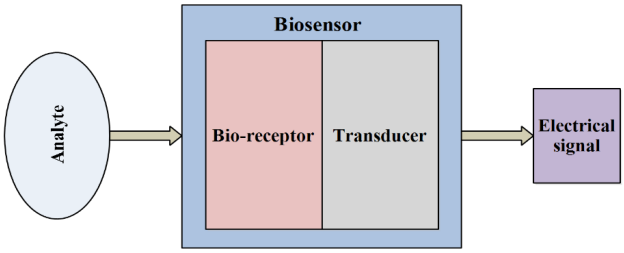

Fig. 1. Basic elements of the biosensor.

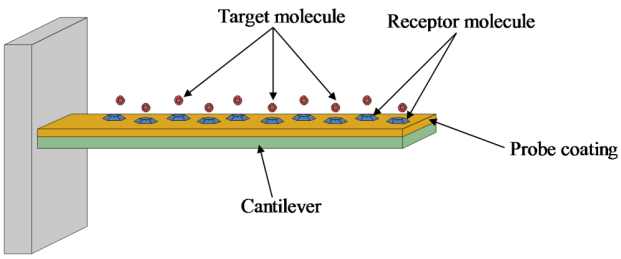

Fig. 2. Detection using a microcantilever.

2.1. Cantilever deflection-based detection

A collected molecule on the active sensing surface of a cantilever could be measured by the deflection of the cantilever due to force made by the adsorption process. Cantilevers are operated in two modes for the measurements: dynamic mode and static mode. In a dynamic mode operation, the absorption of mass on the active sensing surface of a microcantilever beam could result in a noticeable

change in resonance frequency, as the change in mass disturbs the spring constant. In static mode operation, the deflection is the outcome of surface stress differences caused by mass adsorption on the surface of a microcantilever beam on the opposing surface of a cantilever.

2.2. Dynamic mode (analysis based on the change in resonance frequency)

In the dynamic mode, the detection is focused on the variation in the frequency of the cantilever due to the adsorption of mass (Fig. 3). Thermal excitation causes microcantilever beams to resonate freely at their natural frequency. Mass loading decreases the frequency, which allows direct measurement of displacement against its frequency. The quality factor is used to indicate resonance peak sharpness, and individual resonance has a specific quality factor (Q):

$$Q = \frac{2\Delta f}{f_o}, \tag{1}$$

where Δf is the frequency.

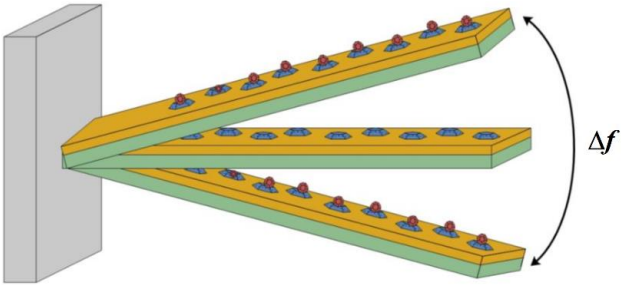

FIG. 3. Dynamic mode detection using microcantilever.

Q factors are responsible for dampening effects from both the geometry and the liquid environment of the cantilever beam, which cause poor resolution in frequency. The higher value of Q-factors allows less minimal detectable resonance shift.

2.3. Static mode (analysis based on the change in displacement)

In static mode, the deflection is the outcome of surface stress differences on the surfaces of the microcantilever beam, which oppose each other (Fig. 4). Variation in stress on surfaces occurs as variations in the energy of surface strain or density occurring due to the absorption of molecules, which minimizes the energy of the surface. A differential surface stress is created by limiting adsorption to one face of a cantilever, causing the bend in the cantilever.

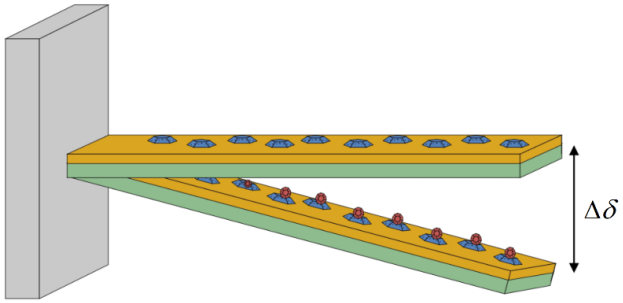

FIG. 4. Static mode detection using microcantilever.

This differential surface stress can be described by Stoney's equation [21]. This equation is a basic expression that relates the stress induced in the material ($\Delta\varepsilon$) per unit length of the material in a film to the curvature (R_k) of the substrate on which the film is deposited. The curvature is independent of the geometrical properties of the film or material. This equation is used in determining the stress induced in the films.

So, the relation is

$$\frac{1}{R_k} = \frac{M}{EI}, \tag{2}$$

where M is the concentrated moment, E is the elastic modulus and I is the moment of inertia for a beam.

The concentrated moment is related to the surface stress and is expressed as

$$M = \frac{WT\Delta\varepsilon}{2}. \tag{3}$$

The moment of inertia is related to the cross-section of a rectangular beam and is expressed as

$$I = \frac{WT^3}{12}, \tag{4}$$

where W is the breadth of the beam, and T is the thickness of the cantilever beam.

Now substituting the values of M and I from Eqs. (3) and (4) into Eq. (2) we obtain:

$$\frac{1}{R_k} = \frac{\frac{WT\Delta\varepsilon}{2}}{E\frac{WT^3}{12}}, \tag{5}$$

$$\frac{1}{R_k} = \frac{6\Delta\varepsilon}{ET^2}. \tag{6}$$

Since L is the length of the beam and R_k is the radius of curvature, then

$$\Delta\delta = \frac{L^2}{2}\left(\frac{1}{R_k}\right). \tag{7}$$

Now substituting the value of $1/R_k$, from Eq. (6) in Eq. (7) we have:

$$\Delta\delta = \frac{L^2}{2}\left(\frac{6\Delta\varepsilon}{ET^2}\right), \tag{8}$$

$$\Delta\delta = \frac{3L^2\Delta\varepsilon}{ET^2}. \tag{9}$$

Since the cantilever is a long and wide-plated type of structure, in general practice, E is changed by the biaxial modulus, i.e., E is be replaced by $\frac{E}{1-\vartheta}$, where ϑ is Poisson's ratio.

So,

$$\Delta\delta = \frac{3L^2\Delta\varepsilon}{\left(\frac{E}{1-\vartheta}\right)T^2}, \tag{10}$$

$$\Delta\delta = \frac{3L^2\Delta\varepsilon(1-\vartheta)}{ET^2}, \tag{11}$$

where $\Delta\delta$ is deflection in the cantilever. This is the well-known form of Stoney's formula.

2.4. Piezoresistive readout technique

Several techniques for measuring cantilever deflection or resonance have been developed in the past decade and have been demonstrated, including optical lever [18], capacitive [19], piezoresistive [13], piezoelectric [13], electron tunneling [18, 20], etc. Piezoresistive readout involves a change in electrical resistance due to deformation. The change in resistance is a combined outcome of material property (i.e., gauge factor) and change in geometry. It exists generally in all types of material. Cantilever movement is sensed by checking the total deformation near the base. This is generally done by just depositing an extra layer on one face of the cantilever.

The fractional change in electrical resistance [25] caused by applied mechanical stress on the material is given by

$$\frac{\Delta R}{R} = (1+2\vartheta)\frac{\Delta l}{l} + \frac{\Delta\rho}{\rho}, \tag{12}$$

where the length of the resistor is l. Under stress for the piezoresistor, the first term of Eq. (12) is negligible compared to the second term.

Thus, Eq. (12) can be rewritten as:

$$\frac{\Delta R}{R} = \frac{\Delta \rho}{\rho}, \tag{13}$$

$$\frac{\Delta \rho}{\rho} = \pi_l \sigma_l + \pi_t \sigma_t, \tag{14}$$

where π_l and π_t are the coefficients of piezoresistivity, longitudinal and transverse, respectively, and σ_l and σ_t are the stresses on piezoresistive material, longitudinal and transverse, respectively. Alternatively, to make it more useful, gauge factor-resistivity can be expressed in terms of strain:

$$\frac{\Delta \rho}{\rho} = \gamma_l \varepsilon_l + \gamma_t \varepsilon_t, \tag{15}$$

where ε_l and ε_t are the longitudinal and transverse strain, respectively, and the longitudinal and transverse elastoresistance coefficients of the material are γ_l and γ_t, respectively.

Now putting the value of $\Delta\rho/\rho$ in Eq. (13) we obtain:

$$\frac{\Delta R}{R} = \gamma_l \varepsilon_l + \gamma_t \varepsilon_t. \tag{16}$$

Now divide Eq. (15) by ε_l, gauge factor (GF):

$$\mathrm{GF} = \frac{\Delta R}{R} / \varepsilon_l = \gamma_l + \gamma_t \frac{\varepsilon_t}{\varepsilon_l}, \tag{17}$$

$$\frac{\Delta R}{R} = \varepsilon_l \mathrm{GF}. \tag{18}$$

Resistance change, $\Delta R/R$, is usually read using the Wheatstone bridge circuit configuration. Four resistors are connected in a loop in Wheatstone bridges, as shown in Fig. 5.

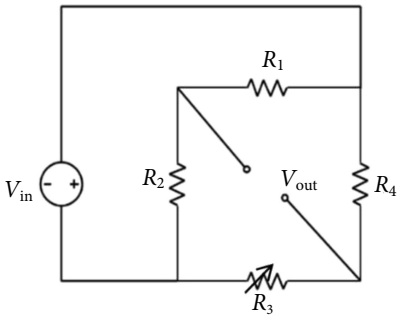

FIG. 5. Piezoresistive readout bridge circuit.

From the above circuit, the output voltage (V_{out}) is:

$$V_{\text{out}} = \left(\frac{R_1}{R_1 + R_2} - \frac{R_4}{R_3 + R_4} \right) V_{\text{in}}. \tag{19}$$

2.5. Antibody-antigen reaction

Antigens are tiny "burglars" that arrive in our bodies and can affect the body. CEA is related to a type of element, known as glycoprotein. It is an early indication of colon cancer. The presence of CEA in the blood of any human is archetypally little. If there is an increase in CEA level in the blood, which is an unusual situation of malignancy, this could indicate a biomarker for a tumor. Bevacizumab [10] is an antibody bound to the CEA antigens. Antibodies layered microcantilever encounter CEA antigen, and the reaction of the antibody-antigen causes an upsurge in mass on the side of the microcantilever biosensor, where the antibody is coated.

3. The design concept of microcantilever

In this section, the steps to design microcantilever-based biosensors are presented as well as an analysis of our proposed design. The COMSOL Multiphysics simulation tool (commercial package) is utilized for all the simulation/experimentation purposes of the designs. There are some steps involved in the designing and analysis process for modeling a design as depicted in Fig. 6.

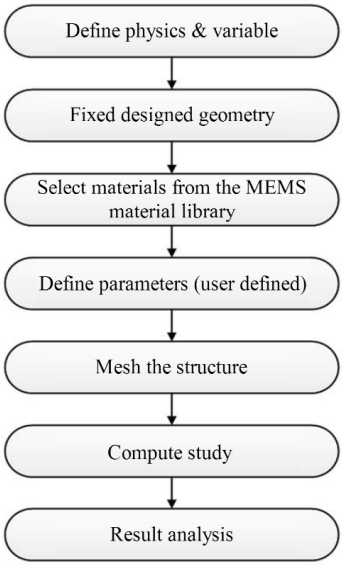

Fig. 6. Modeling process for design geometry.

Firstly, the physics and variables are defined as solid mechanics. Next, we draw our geometry and fix it with different measures and unions. Therefore, the design is completed by defining different work planes and after fixing the designed geometry. Next, different materials are selected from the MEMS material library based on our design requirements. After selecting the materials, some user parameters are chosen and defined based on our parameters criteria. Next, meshing is done using physics-controlled mesh in which finer type is applied for the element size to be precise enough with meshing results. Secondly, the computing is conducted for stationary study type of solid mechanics with the parametric sweep computation, where inputs were selected in a step mode. Lastly, a result analysis is performed, the outputs of the simulation/experimentation, for which the solid surface (3D) output of displacement, von Mises stress, and electric potential modes are studied and the graph analysis of displacement, von Mises stress, and output voltage of terminals are analyzed to the definite results.

3.1. Design parameters

To design the proposed microcantilever, a rectangular-shaped design with length, width, and thickness of 80 μm, 40 μm, and 0.3 μm, respectively, with an active area of 3200 μm^2 is taken as the reference microcantilever. Three designs: Design 1, Design 2, and Design 3 are proposed and for comparing the results with the familiar rectangular-shape design, active area and thickness equivalent to reference (as in rectangular shape) are taken to resemble the proposed design equivalent to the active region (≈ 3200 μm^2). The overall size of the proposed design is defined as 170 μm long and 100 μm wide, which includes the substrate made of a silicon wafer, on which a piezoresistive readout circuit is mounted and has a head protection for the sensing cantilever.

The materials used in the microcantilever-based biosensor design for comparative analysis purposes are listed in Table 1, along with their properties.

Table 1. Various material specifications.

Material	Density [kg/m^3]	Young's modulus [GPa]	Poisson's ratio
GaAs [22]	5320	85.5	0.31
Au [22]	19 280	70	0.44
Polyimide [22]	1300	3.1	0.35
PMMA [23]	1190	3	0.40
Kynar710 [24]	1780	2.3	0.35
Cr [22]	7150	279	0.21
Polysilicon [22]	2300	160	0.22

3.2. Proposed microcantilever beam designs

Solid Mechanics (solid) module and Electric Currents-Single Layer Shell (ecs) module physics of the structural mechanic's mode of COMSOL 5.4 Multiphysics (commercial package) are used to design the microcantilever. These structures of microcantilever beams are designed to study the static displacement analysis. The designed structure is constructed on a silicon wafer with length, width and thickness of 170 μm, 100 μm and 0.3 μm, respectively. The geometry of the proposed constructed microcantilever structures has an active area equivalent to the reference rectangular shape (3200 μm^2) and different materials with different thickness layers, as shown in Fig. 7. The bottom layer is the proposed material, i.e., Kynar710 having a thickness of 300 nm, and then there is a p-silicon single-crystal piezoresistive deposited layer of 200 nm with a doping density of $N_d = 1.32 \times 10^{19}$ $1/cm^3$. Then, the next layer is Kynar710 with a thickness of 30 nm. After that, there is a thin coating of chromium with a thickness of 10 nm, and the top layer is gold with a thickness of 15 nm. The Au/Cr layer is used for better stiffness [2]. So the total thickness of the microcantilever is 0.355 μm and the active sensing area is ≈ 3200 μm^2.

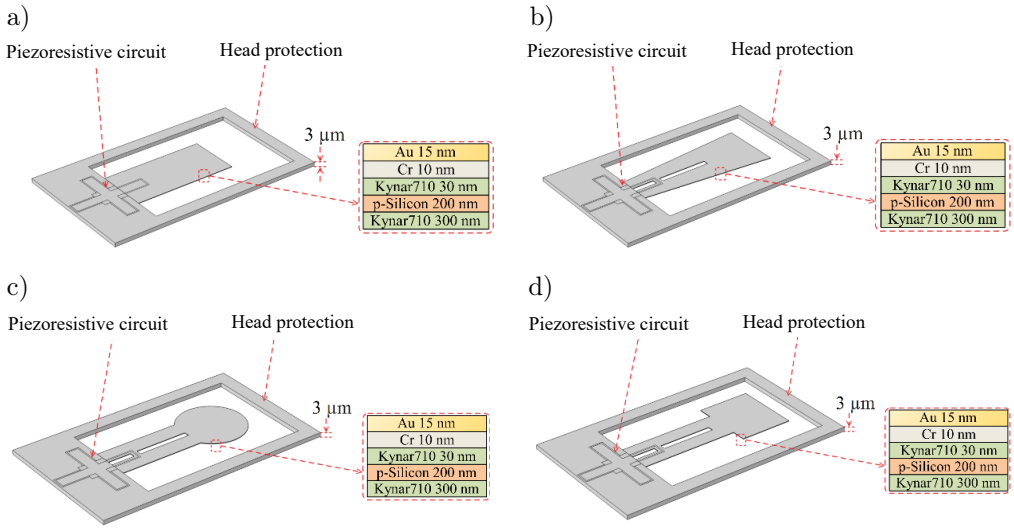

Fig. 7. Schematic 3D-design layout of: a) reference design, b) Design 1, c) Design 2, and d) Design 3 for the detection of CEA.

Geometrical dimensions of the proposed designed structures (shown in Fig. 7) are presented in Fig. 8, and Table 2 shows their parametric values.

A piezoresistive read-out circuit is designed for taking deflection output in terms of millivolt. Geometrical dimensions of piezoresistive readout circuit structures with their parametric values are shown in Fig. 9 and Table 2, respectively.

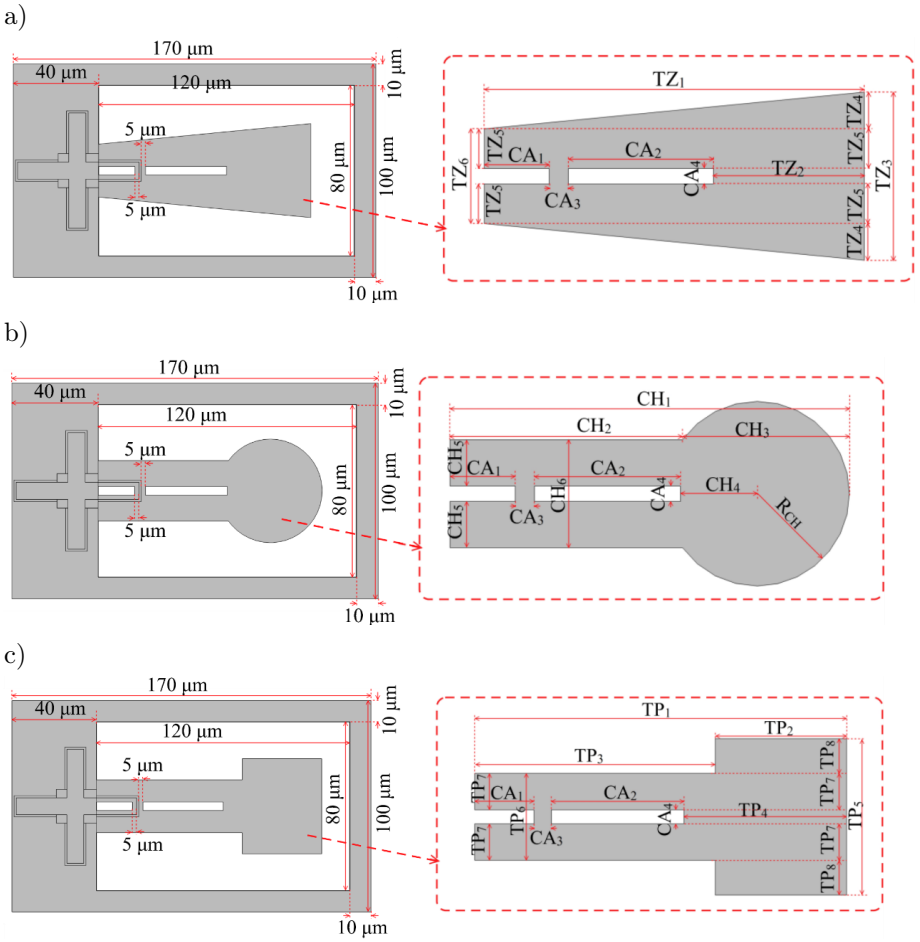

FIG. 8. Geometrical dimension and parameters of: a) Design 1, b) Design 2, and c) Design 3.

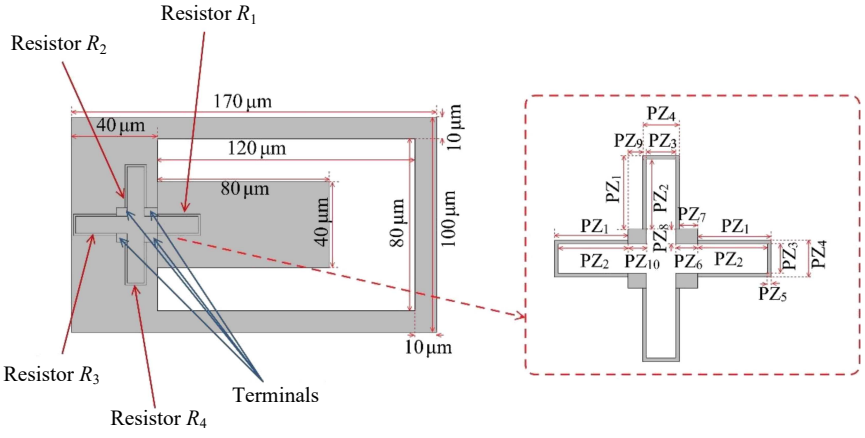

FIG. 9. Piezoresistive readout circuit.

Table 2. Geometrical parametrical values.

Design 1		Design 2		Design 3		Piezoresistive readout circuit	
Dimensional parameters	Values [μm]	Dimensional parameters	Values [μm]	Dimensional parameters	Values [μm]	Dimensional parameters	Values [μm]
CA_1	17	CA_1	17	CA_1	17	PZ_1	20
CA_2	38	CA_2	38	CA_2	38	PZ_2	19
CA_3	5	CA_3	5	CA_3	5	PZ_3	8
CA_4	4	CA_4	4	CA_4	4	PZ_4	10
TZ_1	99.45	CH_1	104	TP_1	106.67	PZ_5	1
TZ_2	39.45	CH_2	60.535	TP_2	37.67	PZ_6	6
TZ_3	44	CH_3	43.465	TP_3	69	PZ_7	5
TZ_4	9.61	CH_4	20	TP_4	46.67	PZ_8	4
TZ_5	10.39	CH_5	12.05	TP_5	45	PZ_9	4
TZ_6	24.78	CH_6	28.08	TP_6	25	PZ_{10}	5
–	–	R_{CH}	24	TP_7	10.5	–	–
–	–	–	–	TP_8	10	–	–

4. Simulation and analysis

4.1. FEM simulation

The design, optimization, and analysis of microcantilever-based biosensors are conducted with the help of the FEM software module. For that, COMSOL 5.4 Multiphysics (commercial package) is used. To form finite elements, the structure is meshed. Parameter values of listed materials are used for designing the structure of the microcantilever beam by using COMSOL Multiphysics software. FEM-based proposed models of Design 1, Design 2, and Design 3 are simulated and designed in the 3D plane of the COMSOL Multiphysics simulator. These designs contain a base made of silicon wafer, which is 170 μm long, 100 μm wide, and 3 μm thick. It has a 120 μm × 80 μm cutting space inside it, as shown in Fig. 7. At the center of the base there is our designed cantilever shown in Fig. 7. Around the sensor, there is a 10 μm wide head protection. One end of the beam is attached to the base and is fixed. There is a piezoresistive-based bridge circuit deposited with four resistors, R_1, R_2, R_3, and R_4. One of the resistors (R_4) is deposited over the microcantilever beam and the remaining four are placed and fixed at the base. The mechanical response and electrical response of the proposed models of designs are achieved by combining Solid Mechanics (solid), Electric Currents-Single Layer Shell (ecs) physics, and Multiphysics of Piezoresistive Effect, Boundary Currents 1 (pzrb1). Piezoresistive material (p-silicon, single-crystal, lightly doped) is used to create the piezoresistive circuit's resistances.

During the study, it is assumed that 1ng of CEA is bound to the microcantilever's surface and it produces 9.8066×10^{-11} Pa pressure [10]. It is found that the molecular weight of CEA is 180 000 Daltons [6],

$$180\,000 \text{ Da } = 2.988 \times 10^{-10} \text{ ng}.$$

We know that 1 ng of CEA is induce a pressure of 9.80665×10^{-11} Pa. So, if assume that 0.1×10^{10} ng of CEA is bound to the microcantilever's surface, the pressure applied equals $0.1 \times 10^{10} \times 9.80665 \times 10^{-11}$ Pa $= 0.098065$ Pa ≈ 0.1 Pa.

Based on the above calculation, a range of 0 to 0.2 Pa pressure is chosen and applied to the microcantilever. The applied pressure acts as the mass of the CEA adsorbed onto the surface of a cantilever beam.

To perform simulation of the proposed microcantilever designs, a rectangular-shaped design having length, width, and thickness of 80 μm, 40 μm, and 0.3 μm, respectively, with an active area of 3200 μm^2 is taken as the reference microcantilever. To form finite elements, the structure is meshed. Parameter values of listed materials are used to design the microcantilever structure of cantilever beam using COMSOL 5.4 Multiphysics (commercial package) software. Material properties of the materials from Table 1 are taken for the simulations. Parametric sweep studies for occurrence and stationery studies for the static mode analysis of the microcantilever are performed to calculate and observe the total deflection of the free end of the devices, von Mises stress at the fixed end of the devices, and the global evaluation of the output voltages of the piezoresistive circuit.

TABLE 3. The total deflection of reference rectangular design caused by different materials [μm].

Materials	Total deflection [μm]
GaAs	0.0049
Au	0.0057
Polyimide	0.0998
PMMA	0.1005
Kynar710	0.1265

4.2. Analysis of proposed designs

To analyze, firstly, the same rectangular shape microcantilever with a sensing area of 3200 μm^2 is taken as reference and the design is tested with different materials, whose properties are listed in Table 2. The calculated pressure range of 0 to 0.2 Pa is applied on the surface of the microcantilever. This pressure range applied acts as the mass of the CEA. The total deflection of the rectangular design (reference) caused by the tested materials is listed in Table 3.

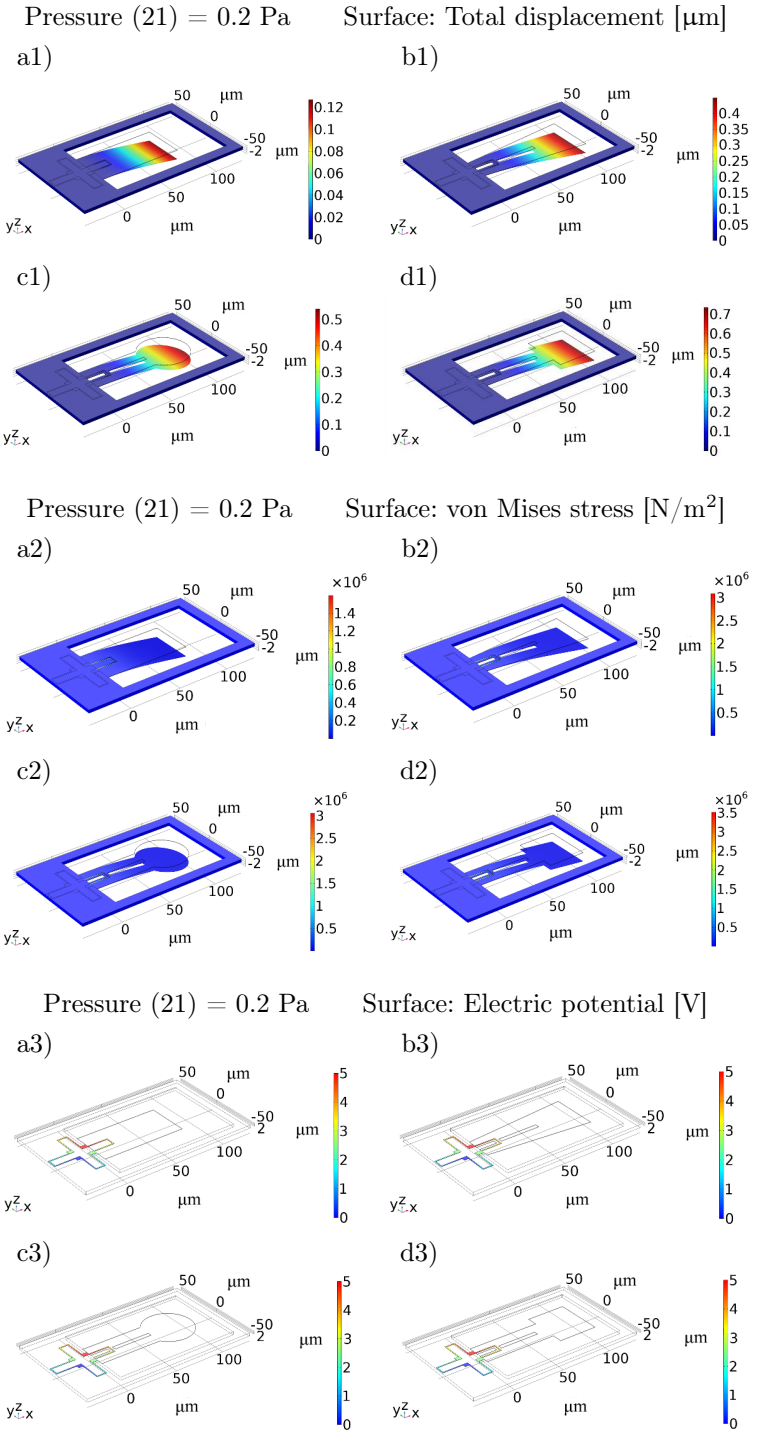

FIG. 10. Simulation of total deflection, von Mises stress and the electric potential of: a1–a3) reference, b1–b3) Design 1, c1–c3) Design 2, d1–d3) Design 3.

The above table clearly states that the material Kynar710 (PVDF) gives the best deflection output in total. Furthermore, three different shape microcantilevers are designed and tested with all the materials, hoping that some other design with different material combinations gives a better result. The analysis of all three proposed designs is done, keeping the same sensing area of 3200 μm^2 is taken as the reference and tested with different materials listed in Table 2.

To investigate the total deflection of the free end of the designed microcantilever, von Mises stress of the fixed end of the designed microcantilever and output voltage due to change in resistance in the piezoresistive readout circuit were investigated. The calculated range of the pressure of 0 to 0.2 Pa was applied on the surface of the microcantilever and a 5V DC voltage was applied at the terminal of the piezoresistive readout circuit. The simulation results using only Kynar710 material are shown in Figs. 10a1–10d3 for different designs.

5. Results and discussion

For better deflection results, the proposed design is simulated with the different materials listed in Table 1. Table 4 shows the total deflection of proposed designs when 0.2 Pa pressure is applied. However, in Table 4 it is observed that the material Kynar710 gives a better result compared to others. In sequence, the proposed designs were tested with all the materials listed in Table 1 by applying the calculated range of pressure from 0 to 0.2 Pa on the surface of the microcantilever, which simulates the mass of the CEA adsorbed onto the surface of a cantilever beam. Figure 11 shows the relation graphs between applied pressure and the corresponding deflection of these proposed designs made with various materials.

Table 4. Total deflection of the proposed designs caused by different materials [μm].

Materials	Proposed designs		
	Design 1	Design 2	Design 3
GaAs	0.0212	0.0188	0.029
Au	0.0253	0.0224	0.0347
Polyimide	0.4201	0.352	0.5702
PMMA	0.4292	0.3591	0.5831
Kynar 710	0.5387	0.4474	0.7328

Here, the graphs of Fig. 11 clearly show that the material Kynar710 gives better performance compared to other materials. Figure 12 shows the relation graphs between applied pressures, corresponding deflection, and output voltages of these proposed designs made with Kynar710.

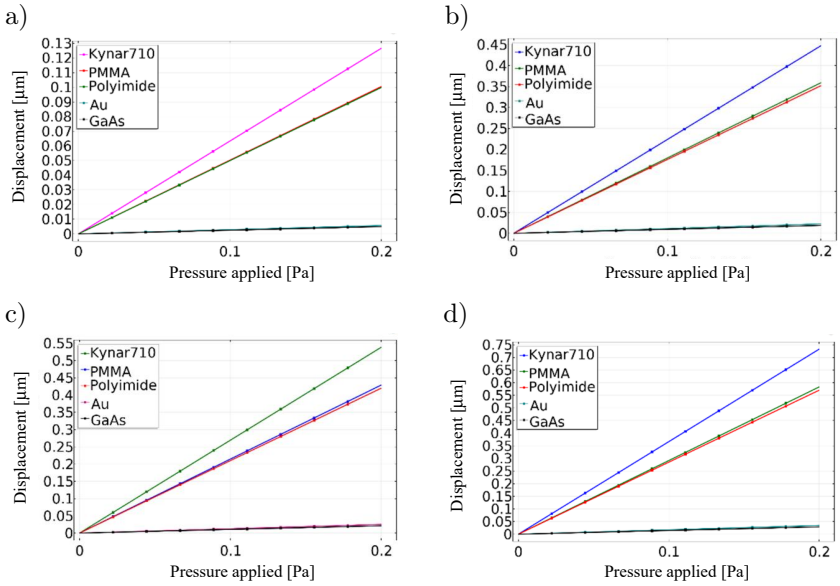

FIG. 11. Applied pressure vs. displacement [µm] graph:
a) reference, b) Design 1, c) Design 2, d) Design 3.

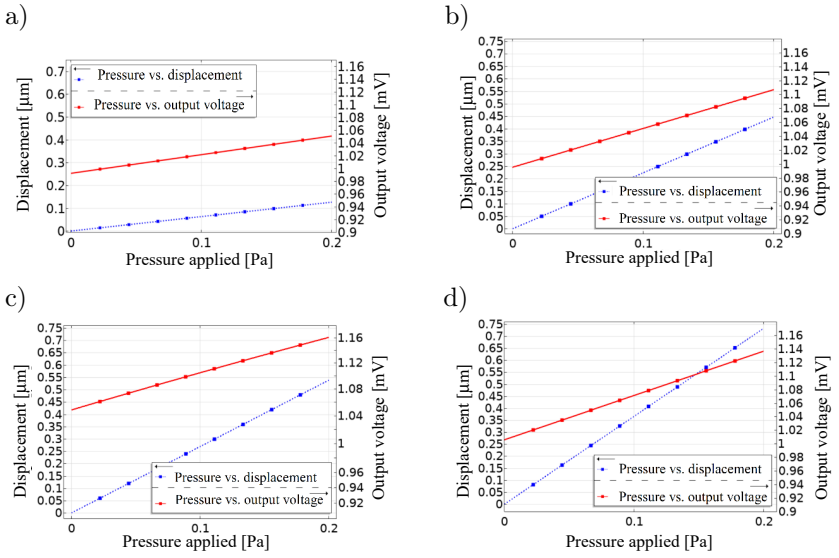

FIG. 12. Applied pressure vs. displacement [µm] vs. output voltage [mV] graph of:
a) reference, b) Design 1, c) Design 2, d) Design 3, using only Kynar710.

In continuation, a comparative analysis of deflection for all the designs was analyzed, which were constructed by Kynar710, for which Fig. 13a shows the deflection comparison with their displacement and Fig. 13b shows the comparison of the slope of output voltage.

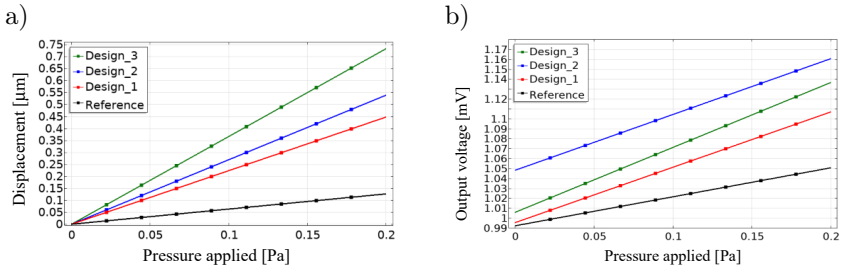

FIG. 13. Comparison graph using all the designs: a) pressure applied vs. displacement [µm], b) pressure applied vs. output voltage [mV].

For the sensitivity analysis, the relative variation in the voltage output per unit of pressure applied from the pressure sensor [17] is

$$S_{\mathrm{Des}} = \frac{\Delta V_{\mathrm{out}}}{P_a} \times \frac{1}{R} = \frac{\Delta V_{\mathrm{out}}}{P_a} \times \frac{1}{V_{\mathrm{in}}}. \tag{20}$$

Based on the data in Table 5, sensitivity was calculated, which is listed in Table 6.

TABLE 5. Output voltage [mV] of all the designs corresponding applied pressure [Pa].

Pressure applied [Pa]	Output voltage [mV]			
	Rectangular reference	Design 1	Design 2	Design 3
0.01	0.995199	1.001049	1.053766	1.012348
0.02	0.998121	1.006628	1.059392	1.018893
0.03	1.001043	1.012206	1.065017	1.025437
0.04	1.003964	1.017785	1.070643	1.031980
0.05	1.006886	1.023363	1.076268	1.038524
0.06	1.009808	1.028942	1.081893	1.045067
0.07	1.012730	1.034520	1.087518	1.051610
0.08	1.015651	1.040098	1.093142	1.058153
0.09	1.018573	1.045676	1.098767	1.064696
0.10	1.021495	1.051254	1.104391	1.071238
0.11	1.024416	1.056832	1.110015	1.077780
0.12	1.027338	1.062409	1.115639	1.084322
0.13	1.030259	1.067987	1.121262	1.090864
0.14	1.033181	1.073564	1.126886	1.097405
0.15	1.036102	1.079141	1.132509	1.103946
0.16	1.039024	1.084718	1.138132	1.110487
0.17	1.041945	1.090295	1.143755	1.117028
0.18	1.044867	1.095872	1.149378	1.123568
0.19	1.047788	1.101449	1.155001	1.130108
0.20	1.050709	1.107025	1.160623	1.136648

Table 6. Sensitivity of proposed designs.

Designs	Sensitivity [(mV/V)/Pa]
Reference	0.058436
Design 1	0.111580
Design 2	0.112519
Design 3	0.130890

6. Conclusion

In this work, three designs of the microcantilever-based biosensor with an equivalent active area of 3200 μm^2 were proposed and tested successfully with Design 1, Design 2 and Design 3 and the FEM analysis of these biosensors was conducted with preciseness using the COMSOL 5.4 Multiphysics (commercial package) software. Designs act as a biosensor for the detection of CEA tumor biomarkers using a microcantilever beam, and an output in terms of displacement as well as in millivolt due to an increase in mass of the CEA adsorbed onto the surface of cantilever beam was observed with proper deflection, which was simulated by applying a pressure in the range of 0 to 0.2 Pa onto the surface of a cantilever beam. A simulation of proposed designs was conducted and experimented with the different materials to obtain better deflection results. The result shows that the reference rectangular design made with Kynar710 showed the best deflection result (i.e., total deflection of 0.1265 μm when 0.2 Pa pressure is applied) compared to other materials. Similarly, a comparison was made with all the designs by utilizing all the materials, in which Design 3 made with Kynar710 gave the highest total deflection of about 0.7328 μm. To get the output in mV, a piezo-resistive bridge circuit made with p-silicon (single-crystal, lightly doped) material was constructed, where one resistor was deposited on the surface of the microcantilever, and 5V was applied to the terminals of the circuit. Depending on the input applied pressure and output mV, the calculation of the sensitivity [(mV/V)/Pa] was checked. Thus, to conclude, based on the experiments, results, and comparisons, Design 3 made with Kynar710 material produced a better sensitivity of about 0.13089 [(mV/V)/Pa] compared to other designs made with various materials.

Acknowledgments

The authors thankfully acknowledge the contributions of MEMS Lab, National Institute of Technology Nagaland, Chumukedima-797103, for providing COMSOL 5.4 Multiphysics (commercial package) software and their extended support.

References

1. D. Di Gioia, I. Blankenburg, D. Nagel, V. Heinemann, P. Stieber, Tumor markers in the early detection of tumor recurrence in breast cancer patients: CA 125, CYFRA 21-1, HER2 shed antigen, LDH, and CRP in combination with CEA and CA 15-3, *Clinica Chimica Acta*, **461**: 1–7, 2016, doi: 10.1016/j.cca.2016.07.014.
2. G. Lech, R. Słotwiński, M. Słodkowski, I.W. Krasnodębski, Colorectal cancer tumour markers and biomarkers: Recent therapeutic advances, *World Journal of Gastroenterology*, **22**(5): 1745–1755, 2016, doi: 10.3748/wjg.v22.i5.1745.
3. P. Gold, S.O. Freedman, Specific carcinoembryonic antigens of the human digestive system, *The Journal of Experimental Medicine*, **122**(3): 467–481, 1965, doi: 10.1084/jem.122.3.467.
4. R.H. Fletcher, Carcinoembryonic antigen, *Annals of Internal Medicine*, **104**(1): 66–73, 1986, doi: 10.7326/0003-4819-104-1-66.
5. C.O. Sahlmann *et al.*, Repeated adjuvant anti-CEA radioimmunotherapy after resection of colorectal liver metastases: safety, feasibility, and long-term efficacy results of a prospective phase 2 study, *Cancer*, **123**(4): 638–649, 2017, doi: 10.1002/cncr.30390.
6. G. Saito, S. Sadahiro, K. Okada, A. Tanaka, T. Suzuki, A. Kamijo, Relation between carcinoembryonic antigen levels in colon cancer tissue and serum carcinoembryonic antigen levels at initial surgery and recurrence, *Oncology*, **91**(2): 85–89, 2016, doi: 10.1159/000447062.
7. K.L.G. Spindler *et al.*, Total cell-free DNA, carcinoembryonic antigen, and C-reactive protein for assessment of prognosis in patients with metastatic colorectal cancer, *Tumor Biology*, **40**(11): 1–8, 2018, doi: 10.1177/1010428318811207.
8. E. Tan, N. Gouvas, R.J. Nicholls, P. Ziprin, E. Xynos, P.P. Tekkis, Diagnostic precision of carcinoembryonic antigen in the detection of recurrence of colorectal cancer, *Surgical Oncology*, **18**(1): 15–24, 2009, doi: 10.1016/j.suronc.2008.05.008.
9. M. Salve, M. Dhone, P. Rewatkar, S. Balpande, J. Kalambe, Design and sensitivity analysis of micro-cantilever based biosensor for tumor detection, *Sensor Letters*, **17**(1): 64–68, 2019, doi: 10.1166/sl.2019.3981.
10. A.M. Upadhyaya, M.C. Srivastava, P. Sharan, Integrated MOEMS based cantilever sensor for early detection of cancer, *Optik*, **227**: 165321, 2021, doi: 10.1016/j.ijleo.2020.165321.
11. W. Xiang, Q. Lv, H. Shi, B. Xie, L. Gao, Aptamer-based biosensor for detecting carcinoembryonic antigen, *Talanta*, **214**: 120716, 2020, doi: 10.1016/j.talanta.2020.120716.
12. C. Li, X. Ma, Y. Guan, J. Tang, B. Zhang, Microcantilever array biosensor for simultaneous detection of carcinoembryonic antigens and α-fetoprotein based on real-time monitoring of the profile of cantilever, *ACS Sensors*, **4**(11): 3034–3041, 2019, doi: 10.1021/acssensors.9b01604.
13. R.M.R. Pinto, V. Chu, J.P. Conde, Label-free biosensing of DNA in microfluidics using amorphous silicon capacitive micro-cantilevers, *IEEE Sensors Journal*, **20**(16): 9018–9028, 2020, doi: 10.1109/JSEN.2020.2986497.
14. G.S. Lakshmi, K.S. Rao, K. Guha, K.G. Sravani, Design of piezoresistive-based microcantilever for MEMS pressure sensor in continuous glucose monitoring system, [in:] *Micro and Nanoelectronics Devices, Circuits and Systems*, pp. 371–379, Springer, Singapore, 2022, doi: 10.1007/978-981-16-3767-4_35.

15. D.R. Rotake, A.D. Darji, Stiffness and sensitivity analysis of microcantilever based piezoresistive sensor for bio-MEMS application, [in:] *2018 IEEE Sensors*, pp. 1–4, IEEE, 2018, doi: 10.1109/ICSENS.2018.8589732.

16. M.A. Andrade *et al.*, A nanomechanical genosensor using functionalized cantilevers to detect the cancer biomarkers miRNA-203 and miRNA-205, *IEEE Sensors Journal*, **20**(6): 2860–2867, 2019, doi: 10.1109/JSEN.2019.2948506.

17. S.S. Kumar, A.K. Ojha, R. Nambisan, A.K. Sharma, B.D. Pant, Design and simulation of MEMS silicon piezoresistive pressure sensor for barometric applications, *Proceedings of the ARTCom&ARTEE PEIE&itSIP and PCIE*, pp. 339–345, Elsevier, 2013.

18. N.V. Lavrik, M.J. Sepaniak, P.G. Datskos, Cantilever transducers as a platform for chemical and biological sensors, *Review of Scientific Instruments*, **75**(7): 2229–2253, 2004, doi: 10.1063/1.1763252.

19. H.P. Lang, C. Gerber, Microcantilever sensors, [in:] *STM and AFM Studies on (Bio)molecular Systems: Unravelling the Nanoworld*, P. Samorì [Ed.], vol. 285, pp. 1–27, Springer, Berlin, Heidelberg, 2008, doi: 10.1007/128_2007_28.

20. D. Rotake, A. Darji, N. Kale, Fabrication, calibration, and preliminary testing of microcantilever-based piezoresistive sensor for BioMEMS applications, *IET Nanobiotechnology*, **14**(5): 357–368, 2020, doi: 10.1049/iet-nbt.2019.0277.

21. U. Eswaran, S. Anand, Design and analysis of high sensitive microcantilever based biosensor for CA 15-3 biomarker detection, *Journal of Applied Science and Computations*, **5**(7): 682–698, 2019, https://www.semanticscholar.org/paper/Design-and-Analysis-of-High-Sensitive-Based-for-CA-Eswaran-Anand/12f1767a37e6c8e6f3a8dbacae7743e676c483fa.

22. A *MEMS Clearinghouse*® and information portal for the MEMS and Nanotechnology community, https://www.memsnet.org/material/.

23. Polymethylmethacrylate (PMMA, Acrylic), MakeItFrom.com, https://www.makeitfrom.com/material-properties/Polymethylmethacrylate-PMMA-Acrylic.

24. CAMPUSplastics, datasheet Kynar® 710, https://www.campusplastics.com/campus/en/datasheet/KYNAR+710/ARKEMA/179/90db57cc.

25. M. Bao, *Analysis and design principles of MEMS devices*, Elsevier, 2005.

Received June 17, 2022; revised version October 2, 2022;
accepted October 31, 2022.